JCTC Journal of Chemical Theory and Computation

Article

pubs.acs.org/JCTC

Applications of Time Dependent and Time Independent Density Functional Theory to the First π to π^* Transition in Cyanine Dyes

Hristina Zhekova,[†] Mykhaylo Krykunov,[†] Jochen Autschbach,[‡] and Tom Ziegler*[,†]

[†]Department of Chemistry, University of Calgary, University Drive 2500, Calgary AB T2N-1N4, Canada

[‡]Department of Chemistry, State University of New York, 312 Natural Sciences Complex, Buffalo, New York 14260-3000, United States

ABSTRACT: The first $\pi \rightarrow \pi^*$ transition in a number of cyanine dyes was studied using both time dependent and time independent density functional methods using a coupled cluster (CC2) method as the benchmark scheme. On the basis of 10 different functionals, it was concluded that adiabatic time dependent density functional theory (ATDDFT) almost independently of the functional gives rise to a singlet−triplet separation that is too large by up to 1 eV, leading to too high singlet energies and too low triplet energies. This trend is even clearer when the Tamm−Dancoff (TD) approximation is introduced and can in ATDDFT/TD be traced back to the representation of the singlet−triplet separation by a HF-type exchange integral between π and π^*. The time independent DFT methods (ΔSCF and RSCF-CV-DFT) afford triplet energies that are functional independent and close to those obtained by ATDDFT. However, both the singlet energies and the singlet−triplet separations increases with the fraction α of HF exchange. This trend can readily be explained in terms of the modest magnitude of a KS-exchange integral between π and π^* in comparison to the much larger HF-exchange integral. It was shown that a fraction α of 0.5 affords good estimates of both the singlet energies and the singlet−triplet separations in comparison to several *ab initio* benchmarks.

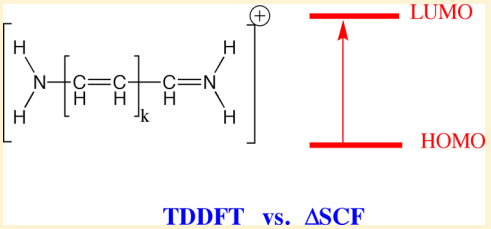

1. INTRODUCTION

Excited states can be described by methods that are based on either response theory or variational schemes.[1,2] In wave function quantum mechanics, both approaches have led to procedures that are highly accurate for organic molecules.[3] The accurate wave function schemes scale as n^6 with the number of electrons. They are thus relatively expensive for larger systems, although attempts are underway to introduce a more favorable scaling.[4−6]

Within DFT, excited states have primarily been dealt with by approaches based on response theory such as time dependent DFT (TDDFT).[7,8] This is understandable since DFT in its traditional formulation is a ground state theory. Further, TDDFT represents an attractive compromise between computational speed and accuracy with its favorable scaling as n^4 or less. Nevertheless, variational DFT approaches have also been used with some success. Perhaps the best known is the ΔSCF scheme by Slater and Wood.[9]

Both DFT and TDDFT can be formulated as exact theories. However, their practical applications are based on simplifications. For TDDFT, they involve the employment of approximate functionals as well as the adiabatic approximation.[10] Challenging problems for TDDFT have been charge transfer and Rydberg transitions[11−15] as well as single electron excitations with some double transition character where one has to go beyond the adiabatic approximation (ATDDFT).[16−27] Another problematic case for TDDFT has been the simple cyanine dyes, which will be the subject of this investigation.[28−41]

We have recently developed a constricted variational DFT method (CV-DFT)[42−45] for the description of excited states. In CV-DFT, we allow the occupied ground state orbitals $\{\phi_i(1); i = 1, \text{occ}\}$ to vary by mixing into each $\phi_i(1)$ a fraction of every virtual ground state orbital $\{\phi_a(1); a = 1, \text{vir}\}$ according to $\delta\phi_i \propto \Sigma_a U_{ai}\phi_i$. The resulting energy can be evaluated to any desired order in U_{ai}. Further, the mixing coefficients U_{ai} can be optimized variationally. It has previously been shown[44−47] that the variational CV-DFT approach to second order in U_{ai} is equivalent to adiabatic TDDFT based on response theory within the Tamm−Dancoff approximation.[48] Further, CV-DFT is able to treat charge transfer transitions[46,47] even with local functionals when terms to all orders in U_{ai} are taken into account. However, this requires that U_{ai} is fully optimized[43] and that the basis of occupied $\{\phi_i(1); i = 1, \text{occ}\}$ and virtual $\{\phi_a(1); a = 1, \text{vir}\}$ ground state orbitals is allowed to relax (RSCF-CV(∞)-DFT)[42]

The objective of the current investigation is to study the performance of RSCF-CV(∞)-DFT or the kindred ΔSCF as applied to simple cyanine dyes compared to adiabatic TDDFT[28−31] for a number of functionals. We shall use recent *ab initio* calculations as benchmarks and study the performance of the different DFT based methods for singlet as well as triplet excitations.

Received: April 5, 2014

   dx.doi.org/10.1021/ct500292c | *J. Chem. Theory Comput.* XXXX, XXX, XXX−XXX

2. THEORETICAL DETAILS

The RSCF-CV(∞)-DFT scheme[42] has already been described in great detail for single electron transitions elsewhere. Nevertheless, we shall here sketch the part of the theory that will be important for the analysis of our calculations on the first π to π^* transition in cyanine dyes.

2.1. The RSCF-CV-DFT Scheme. In the self-consistent formulation of constricted variational density functional theory with orbital relaxation included (RSCF-CV-DFT),[42] excited state KS orbitals are constructed by performing a unitary transformation among a set of relaxed occupied

$$\psi_i'(1) \to \phi_i(1) + \sum_c^{\text{vir}} R_{ci}\phi_c(1) - \frac{1}{2}\sum_c^{\text{vir}}\sum_k^{\text{occ}} R_{ci}R_{ck}\phi_k(1) + O^{(3)}[R] \tag{1}$$

and unoccupied reference orbitals

$$\psi_a'(1) \to \phi_a(1) - \sum_k^{\text{vir}} R_{ak}\phi_k(1) - \frac{1}{2}\sum_c^{\text{vir}}\sum_k^{\text{occ}} R_{ak}R_{ck}\phi_c(1) + O^{(3)}[R] \tag{2}$$

Here, $\{\phi_k; k = 1, \text{occ}\}$ and $\{\phi_a; a = 1, \text{vir}\}$ are, respectively, the occupied and virtual canonical orbitals from a ground state calculation and R is a matrix that relaxes these orbitals by mixing $\{\phi_k; k = 1, \text{occ}\}$ and $\{\phi_a; a = 1, \text{vir}\}$ to produce the reference sets $\{\psi_k; k = 1, \text{occ}\}$ and $\{\psi_a; a = 1, \text{vir}\}$. In evaluating the corresponding relaxation energy terms up to second order in R are taken into account.[42]

The unitary transformation among the reference orbitals reads

$$Y\begin{pmatrix}\psi_{\text{occ}}\\ \psi_{\text{vir}}\end{pmatrix} = e^{U}\begin{pmatrix}\psi_{\text{occ}}\\ \psi_{\text{vir}}\end{pmatrix} = \left(\sum_{m=0}^{\infty}\frac{(U)^m}{m!}\right)\begin{pmatrix}\psi_{\text{occ}}\\ \psi_{\text{vir}}\end{pmatrix} = \begin{pmatrix}\psi_{\text{occ}}'\\ \psi_{\text{vir}}'\end{pmatrix} \tag{3}$$

and is in CV(n)-DFT carried out to order n in U.[42]

Here, ψ_{occ} and ψ_{vir} are concatenated column vectors containing the sets of occupied $\{\psi_i; i = 1, \text{occ}\}$ and virtual $\{\psi_a; a = 1, \text{vir}\}$ ground state reference orbitals defined above, whereas ψ_{occ}' and ψ_{vir}' are concatenated column vectors containing the resulting sets $\{\psi'; i = 1, \text{occ}\}$ and $\{\psi'_a; a = 1, \text{vir}\}$ of occupied and virtual orbitals corresponding to the single electron transition. The unitary transformation matrix Y is, in eq 1, expressed in terms of a skew symmetric matrix U as

$$\begin{aligned} Y &= e^{U} \\ &= I + U^I + \frac{(U)^2}{2} + \dots \\ &= \sum_{m=0}^{\infty}\frac{(U)^m}{m!} \\ &= \sum_{m=0}^{\infty}\frac{((U)^2)^m}{2m!} + U\sum_{m=0}^{\infty}\frac{((U)^2)^m}{(2m+1)!} \end{aligned} \tag{4}$$

The first occ elements in any row or column of U run over occupied ground state reference orbitals starting with those of α-spin. Likewise, the last vir elements run over virtual ground state reference orbitals ending with those of β-spin. Further, $U_{ij} = U_{ab} = 0$, where "i,j" refers to the occupied set $\{\psi_i; i = 1, \text{occ}\}$, whereas "$a,b$" refers to $\{\psi_a; a = 1, \text{vir}\}$. Here, U_{ai} are the variational mixing matrix elements that combine virtual and occupied ground state orbitals in the excited state with $U_{ai} = U_{ia}$. Thus, the entire matrix $U_{ai} = U_{ia}$ is made up of occ × vir independent elements U_{ai} that also can be organized in the column vector $\vec{U}$ where the running index now is the number of different occ/vir pairs (a, i). For a given $\vec{U}$, we can, by the help of eq 4, generate a set of "occupied" excited state orbitals

$$\psi_i' = \sum_p^{\text{occ+vir}} Y_{pi}^i\psi_p = \sum_j^{\text{occ}} Y_{ji}^i\psi_j + \sum_a^{\text{vir}} Y_{ai}^i\psi_a \tag{5}$$

that are orthonormal to order n in U_{ai}. Summing up all orders in U, the occupied excited state orbitals from the unitary transformation eq 2 can be written in a compact form[42−45] as

$$\psi_i^i = \cos[\gamma_i]\psi_{i_o} + \sin[\gamma_i]\psi_{i_v} \tag{6}$$

Here,[42−45] $\gamma_i(i = 1, \text{occ})$ is a set of eigenvalues to

$$(\mathbf{V}^I)^+\mathbf{U}^I\mathbf{W}^I = 1\gamma^I \tag{7}$$

,where γ is a diagonal matrix of dimension occ. Further

$$\psi_{i_o} = \sum_j^{\text{occ}} (W)_{ji}\psi_j \tag{8}$$

and

$$\psi_{i_v} = \sum_b^{\text{vir}} (V)_{bi}\psi_b \tag{9}$$

where i, j run over the occupied ground state orbitals and b over the virtual ground state orbitals. The orbitals defined in eqs 6−9 were first introduced by Amos and Hall[49] as the corresponding occupied and virtual orbital pair that is mixed in the unitary transformation defined by U. They have been explored in connection with electron excitations as *Natural Transition Orbitals* (NTO) by Martin[50] since they give a more compact description of the excitations than the canonical orbitals. Thus, a transition that involves several $i \to j$ replacements among canonical orbitals can often be described by a single replacement $\psi_{i_o} \to \psi_{i_v}$ in terms of NTOs. In that case, $\gamma_j^I = \pi/2$ for $j = i$, whereas $\gamma_j^I = 0$ for $j \neq i$.[50]

In the procedure above, we started with the ground state KS-determinant

$$\Psi^0 = |\phi_1\phi_2\phi_3\dots\phi_i\phi_j\dots\phi_n| \tag{10}$$

and generated the KS determinant for the one-electron transition.

$$\Psi' = |\psi_1'\psi_2'\psi_3'\dots\psi_i'\psi_j'\dots\psi_n'| \tag{11}$$

From eqs 1,2,5 we can now express the KS energy of Ψ' as

$$E' = E^0 + \Delta E'(R, U) \tag{12}$$

to second order in R and nth order in U. Further, in RSCF-CV(n)-DFT, the two matrices R and U are determined self-consistently under the constraint (constriction) that the excitation I represents a transfer of one electron from the density space described by the occupied reference orbitals $\{\psi_i; i = 1, \text{occ}\}$ to that and virtual $\{\psi'_a; a = 1, \text{vir}\}$.

2.2. The Relation Between Adiabatic Time Dependent DFT and the RSCF-CV(n)-DFT Method. We shall in our discussion of the first π to π^* transition in cyanine dyes make use of two limiting cases for the RSCF-CV(n)-DFT scheme. The first is adiabatic time dependent DFT within the Tamm-

dx.doi.org/10.1021/ct500292c | J. Chem. Theory Comput. XXXX, XXX, XXX−XXX

Dancoff approximation[48] (ATDDFT/TD) which is equivalent to CV(2)-DFT.[43−45] In this scheme the excited state KS-orbitals are given by.[45]

$$\psi_i'(1) \rightarrow \psi_i(1) + \sum_c^{\text{vir}} U_{ci}\psi_c(1) - \frac{1}{2}\sum_c^{\text{vir}}\sum_k^{\text{occ}} U_{ci}U_{ck}^*\psi_k(1) + O^{(3)}[U] \tag{13}$$

The corresponding energy to second order in U can be written as[45]

$$\Delta E^{(2)} = \sum_i^{\text{occ}}\sum_a^{\text{vir}} U_{ai}U_{ai}[\varepsilon_a(\rho^0) - \varepsilon_i(\rho^0)] + \sum_i^{\text{occ}}\sum_a^{\text{vir}}\sum_j^{\text{occ}}\sum_b^{\text{vir}} U_{ai}U_{bj}K_{ai,bj} \tag{14}$$

Here, $\varepsilon_a(\rho^0)$ and $\varepsilon_i(\rho^0)$ are the ground state orbital energies for ψ_a and ψ_i, respectively. Further

$$K_{pq,st} = K^{\text{C}}_{pq,st} + K^{\text{XC}}_{pq,st} \tag{15}$$

with

$$K^{\text{C}}_{pq,st} = \int\int \psi_p(1)\,\psi_q(1)\frac{1}{r_{12}}\,\psi_s(2)\,\psi_t(2)\,\mathrm{d}v_1\,\mathrm{d}v_2 \tag{16}$$

In addition $K^{\text{XC}}_{pq,st}$ is given by

$$K^{\text{XC(HF)}}_{pq,st} = -\int\int \psi_p(1)\,\psi_s(1)\frac{1}{r_{12}}\,\psi_q(2)\,\psi_t(2)\,\mathrm{d}v_1\,\mathrm{d}v_2 \tag{17}$$

for Hartree−Fock exchange-correlation and by

$$K^{\text{XC(KS)}}_{pq,st} = \int \psi_p^{\mu}(\vec{r}_1)\,\psi_q^{\mu}(\vec{r}_1)\,f^{\mu\nu}(\vec{r}_1)\,\psi_s^{\nu}(\vec{r}_1)\,\psi_t^{\nu}(\vec{r}_1)\,\mathrm{d}\vec{r}_1 \tag{18}$$

for local KS exchange correlation. The integration in eqs 16 and 17 is over space and spin, whereas it is over space only in eq 18. The factor $f^{\mu\nu}(\vec{r}_1)$ in eq 18 represents the regular energy kernel

$$f^{\mu\nu} = \left(\frac{\delta^2 E_{\text{XC}}}{\delta\rho^{\mu}\delta\rho^{\nu}}\right)_0 \tag{19}$$

given by the functional derivative of E_{XC} with respect to the density of electrons of μ,ν spin taken at the ground state reference. If μ and ν represent opposite spin, we write the corresponding K and $K^{\text{XC(KS)}}$ integrals with "bars" as $K_{pq,\bar{s}\bar{t}}$ and $K^{\text{XC(KS)}}_{pq,\bar{s}\bar{t}}$, respectively. The "bars" are omitted if μ,ν comes from spin−orbitals with the same spin.

For excitations involving a single orbital replacement $(i \rightarrow a)$, we get for the triplet excitation energy

$$\Delta E_T^{\text{CV(2)}} = [\varepsilon_a(\rho^0) - \varepsilon_i(\rho^0)] + K_{aiai} - K_{ai\bar{a}\bar{i}} \tag{20}$$

whereas the singlet excitation energy is given by

$$\Delta E_{\text{S}}^{\text{CV(2)}} = [\varepsilon_a(\rho^0) - \varepsilon_i(\rho^0)] + K_{aiai} + K_{ai\bar{a}\bar{i}} \tag{21}$$

and the triplet-singlet separation by

$$\begin{aligned}\Delta E_{\text{S/T}}^{\text{CV(2)}} &= \Delta E_{\text{S}}^{\text{CV(2)}} - \Delta E_{\text{T}}^{\text{CV(2)}} \\ &= 2K_{ai\bar{a}\bar{i}} \\ &= 2K^{\text{C}}_{aiai} + 2K^{\text{XC}}_{ai\bar{a}\bar{i}} \\ &\approx \Delta\tilde{E}_{\text{S/T}}^{\text{CV(2)}} \\ &= 2K^{\text{C}}_{aiai}\end{aligned} \tag{22}$$

Here, $\approx$ indicates that $2K^{\text{XC}}_{ai\bar{a}\bar{i}}$ is either zero for HF or small for KS. Thus, $\Delta\tilde{E}_{\text{S/T}}^{\text{CV(2)}}$ of eq 22 is determined by the Coulomb (but exchange type) integral $2K^{\text{C}}_{aiai}$ that has the same form for HF and KS and thus only depends indirectly on the functional through the shape of the orbitals as pointed out by Casida[8] and others.[31]

The triplet transition energy for an excitation that can be represented by a single orbital replacement $(i \rightarrow a)$ takes on the form

$$\Delta E_{\text{T}}^{\text{CV}(\infty)} = [\varepsilon_a(\rho^0) - \varepsilon_i(\rho^0)] + \frac{1}{2}K_{aaaa} + \frac{1}{2}K_{iiii} - K_{aa\bar{i}\bar{i}} + \Delta E^{\text{T}}_{\text{Rel}}(R) \tag{23}$$

for the all order RSCF-CV(∞)-DFT method.[42] Here, $\Delta E^{T}_{\text{Rel}}(R)$ is the orbital relaxation energy for RSCF-CV(∞)-DFT. This energy is zero for the CV(2) method.

The corresponding singlet energy is given by

$$\Delta E_{\text{S}}^{\text{CV}(\infty)} = [\varepsilon_a(\rho^0) - \varepsilon_i(\rho^0)] + \frac{1}{2}K_{aaaa} + \frac{1}{2}K_{iiii} - 2K_{aaii} + K_{aa\bar{i}\bar{i}} + \Delta E^{\text{S}}_{\text{Rel}}(R) \tag{24}$$

whereas the singlet−triplet separation takes on the form

$$\begin{aligned}\Delta E_{\text{S/T}}^{\text{CV}(\infty)} &= \Delta E_{\text{S}}^{\text{CV}(\infty)} - \Delta E_{\text{T}}^{\text{CV}(\infty)} \\ &= -2K_{aaii} + 2K_{aa\bar{i}\bar{i}} + \Delta E^{\text{S}}_{\text{Rel}}(R) - \Delta E^{\text{T}}_{\text{Rel}}(R) \\ &\approx -2K^{\text{XC}}_{aaii}\end{aligned} \tag{25}$$

where $\approx$ again means that in a qualitative discussion of our quantitative calculations with all terms included, we can neglect $\Delta E^{\text{S}}_{\text{Rel}}(R) - \Delta E^{\text{T}}_{\text{Rel}}(R)$ and $2K^{\text{XC}}_{aa\bar{i}\bar{i}}$. For functionals with a fraction $\alpha(0.0 \le \alpha \le 1.0)$ of HF-exchange, we get

$$\begin{aligned}\Delta\tilde{E}_{\text{S/T}}^{\text{CV}(\infty)} &= -2K^{\text{XC(Hyb)}}_{aaii} \\ &= -2(1-\alpha)K^{\text{XC(KS)}}_{aaii} - 2\alpha K^{\text{XC(HF)}}_{aaii} \\ &= -2(1-\alpha)K^{\text{XC(KS)}}_{aaii} + 2\alpha K^{\text{C}}_{aiai}\end{aligned} \tag{26}$$

Thus, since from observations

$$0.0 < -K^{\text{XC(KS)}}_{aaii} < K^{\text{C}}_{aiai} \tag{27}$$

we find in general $\Delta\tilde{E}_{\text{S/T}}^{\text{CV}(\infty)} < \Delta\tilde{E}_{\text{S/T}}^{\text{CV(2)}}$ for pure DFT. However, as the fraction α of HF-exchange increases, the difference decreases until pure HF with $\alpha = 1$ where $\Delta\tilde{E}_{\text{S/T}}^{\text{CV}(\infty)} = \Delta\tilde{E}_{\text{S/T}}^{\text{CV(2)}}$. Thus, $\Delta\tilde{E}_{\text{S/T}}^{\text{CV}(\infty)}$ is strongly functional dependent in contrast to $\Delta\tilde{E}_{\text{S/T}}^{\text{CV(2)}}$.[31] We shall make use of this later on.

3. COMPUTATIONAL DETAILS

All calculations were based on DFT as implemented in a developers version of the ADF 2012 program.[51] Our calculations employed a standard triple-ζ Slater type orbital (STO) basis with two sets of polarization functions for all atoms.[52] Use was made of the local density approximation in

dx.doi.org/10.1021/ct500292c | J. Chem. Theory Comput. XXXX, XXX, XXX−XXX

the VWN parametrization[53] and the BP86 generalized gradient approximation (GGA) with the correlation part by Perdew and Wang[54] and the exchange part by Becke.[55] We employed further the B3LYP and BH&HLYP (BHLYP) hybrid functionals of Becke[56] with the correlation functional taken from Lee et al.[57] Here, B3LYP has 20% Hartree−Fock exchange, whereas the fraction is 50% for BHLYP. Employed as well was the PBE[58] and PBE0[59,60] functionals where the latter has 25% HF exchange.

Use has also been made of length corrected functionals (LC).[12−15,61] In the LC functional, the regions of electron−electron interaction are divided into "long-" and "short-"range parts by dividing the Coulomb operator into two pieces:

$$1/r_{12} = \mathrm{SR} + \mathrm{LR} = \frac{w(\omega, r_{12})}{r_{12}} + \frac{1 - w(\omega, r_{12})}{r_{12}} \tag{28}$$

where r_{12} is the interelectronic distance $r_{12} = |\vec{r}_1 - \vec{r}_2|$, whereas w is some kind of continuous switching function that goes to 1 as r_{12} goes to zero and to zero as r_{12} becomes large. The parameter ω determines how rapidly the switching occurs. This type of division has been introduced by a number of groups to combine DFT and wave function theory.[59] The most widely used form for $w(\omega, r_{12})$ is the error function[62,63] as it gives rise to integrals that are readily evaluated in connection with Gaussian basis sets. An alternative choice is the exponential function

$$w(\omega, r_{12}) = \exp(-\omega r_{12}) \tag{29}$$

which in combination with the r_{12}^{-1} operator gives the Yukawa potential.[63] The exponential choice for $w(\omega, r_{12})$ in eq 29 has been used for both Gaussian[62,63] and Slater type basis sets.[64,65] We employ here $w(\omega, r_{12})$ in eq 29 with $\omega = 0.40$ and $\omega = 0.75$ when nothing else is mentioned. The local functional used in conjunction with LC was BP86. Here, LC combined with BP86 for $\omega = 0.40$ is termed LCBP86, whereas the combination with $\omega = 0.75$ is called LCBP86′. We have finally also included the LC functional CAMB3LYP.[66]

All electrons were treated variationally without the use of the frozen core approximation.[51] The parameter for the precision of the numerical integration was set to a (standard) value of 4.0. A special auxiliary STO basis was employed to fit the electron density in each cycle for an accurate representation of the exchange and Coulomb potentials.[51] All structures shown in Figure 1 were taken from ref 31 with the exception of $k = 0$ (CN3), where the geometry was optimized in C_{2v} symmetry using PBE0 and the triple-ζ basis mentioned above.

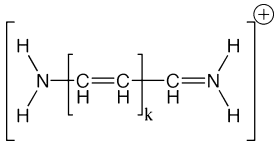

Figure 1. Cyanine model.

4. RESULTS AND DISCUSSION

The first singlet $\pi \rightarrow \pi^*$ excitation in cyanine dyes has been studied extensively. Schreiber[27] et al. found in their 2001 CASPT2 investigation excitation energies that were well above experimental values but below TDDFT results, Table 1. They explained the deviation from experimental values with solvent effects not taken into account in their gas phase calculations. The authors pointed out at the same time that gas-phase TDDFT apparently has a problem with cyanine dyes since the calculated first $\pi \rightarrow \pi^*$ singlet excitation energies systematically are overestimated. More recently, better *ab initio* benchmark calculations based on an improved CASPT2 treatment[29] as well as extrapolated coupled cluster response theory (exCC3)[29] and a dynamic Monte Carlo[29] simulation have appeared. They raise the values of the best estimates for the singlet excitations so that they now are closer to the estimate obtained by the most advanced TDDFT methods,[28−30] Table 1. Thus, TDDFT might be "not guilty"[30] of large errors for cyanines as initially alleged.[27] Nevertheless, it can still be concluded[31] that cyanine singlet $\pi \rightarrow \pi^*$excitation energies calculated by TDDFT are overestimated, a trend that becomes even clearer when use is made of the TD approximation.[48] The reason for this has in part been attributed to an error in the differential correlation between the ground and excited states.[28,31]

We shall in the first part of our study provide a new angle on the performance of TDDFT for cyanines by analyzing how the deviations of the singlet transition energies are determined by errors in the corresponding triplet energies and singlet−triplet separations determined by TDDFT (and TDDFT/TD). In the second part, we apply the RSCF-CV(∞)-DFT (or ΔSCF) method to the cyanines using the same functionals as for TDDFT. The emphasis now is not only on the ability of RSCF-CV(∞)-DFT to determine singlet transition energies but also on its performance with respect to triplets and singlet−triplet separation energies.

4.1. TDDFT Excitation Energies. We display in Figure 2 the calculated triplet TDDFT $\pi \rightarrow \pi^*$ excitation energies for CN($2m + 1$) ($m = 1, 5$) based on seven different functionals: LDA, BP86, PBE, B3LYP, PBE0, BHLYP, and M06. The triplet excitation energies are only moderately functional dependent with a slight tendency toward lower values as the fraction (α) of HF exchange increases. The TDDFT triplet excitation energies are further seen to be too low compared to the best available estimate (Best) based on CC2 calculations[31] with an average deviation close to 0.4 eV. Further, the local functionals perform better than the hybrids with a large portion (α) of HF exchange.

The $\pi \rightarrow \pi^*$ excitations studied here involve essentially a single orbital replacement. As a consequence, their excitation energy can be written within the TD approximation according to eq 20 as

$$\begin{aligned}\Delta E_{\mathrm{T}}^{\mathrm{CV}(2)} &= [\varepsilon_{\pi^*}(\rho^0) - \varepsilon_{\pi}(\rho^0)] + K_{\pi^*\pi\pi^*\pi} - K_{\pi^*\pi\bar{\pi}^*\bar{\pi}} \\ &\approx [\varepsilon_{\pi^*}(\rho^0) - \varepsilon_{\pi}(\rho^0)] + (1 - \alpha)K_{\pi^*\pi\pi^*\pi}^{\mathrm{XC(KS)}} \\ &\quad + \alpha K_{\pi^*\pi\pi^*\pi}^{\mathrm{XC(HF)}}\end{aligned} \tag{30}$$

We plot $\Delta E_{\mathrm{T}}^{\mathrm{CV}(2)}$ (or TDDFT/TD) in Figure 3 for different functionals in the case of CN3. The triplet energies are again nearly functional independent. This is in spite of the fact that both $[\varepsilon_{\pi^*}(\rho^0) - \varepsilon_{\pi}(\rho^0)]$ and $K_{\pi^*\pi\pi^*\pi} - K_{\pi^*\pi\bar{\pi}^*\bar{\pi}}$ exhibit a strong dependence on the fraction (α) of HF exchange, Figure 3. Apparently, this dependence disappears in the difference. Without the TD approximation, the triplet energy expression for pure TDDFT becomes slightly more complex.[31] The biggest difference in numerical terms is that $\Delta E_{\mathrm{T}}^{\mathrm{TDDFT}}$ for a large fraction (α) of HF exchange drops below $\Delta E_{\mathrm{T}}^{\mathrm{CV}(2)}$. This drop can be considerable and will in some cases artificially place the triplet below the true singlet ground state causing a triplet

dx.doi.org/10.1021/ct500292c | J. Chem. Theory Comput. XXXX, XXX, XXX−XXX

Table 1. Benchmark *ab Initio* Singlet Excitation Energies (eV) Compared to TD-DFT Results and Experiment

	CASPT2[a]	CASPT2-IPEA[b]	DMC[c]	exCC3[d]	PBE0[e]	PBE0-TDA[e]	B2PLYP[f]	M06-2X[g]	ΔSCF[h]	expt[i]
CN3	6.63	7.20	7.36	7.16	7.62	8.03	7.30		7.33	5.54
CN5	4.36	4.69	5.03	4.84	5.33	5.84	5.05	5.33	4.81	3.99
CN7	3.22	3.53	3.82	3.65	4.18	4.71	3.92	4.17	3.55	2.98
CN9	2.56	2.81	3.09	2.96	3.50	4.02	3.25	3.47	2.79	2.39
CN11	2.12	2.46	2.62	2.53	3.03	3.54	2.80	3.00	2.29	1.98

[a]Complete active space second order perturbation theory calculation from ref 27. [b]CASPT2 calculations, with ionization potential-electron affinity (IPEA) shifts according to ref 29. [c]Diffuse Monte Carlo calculations from ref 29. [d]Response based extrapolated coupled cluster calculation from ref 29. [e]Ref 29. [f]Double hybride DFT from ref 28. [g]Minnesota type functional with 54% exchange from ref 30. [h]Based on BHLYP. [i]Ref 67.

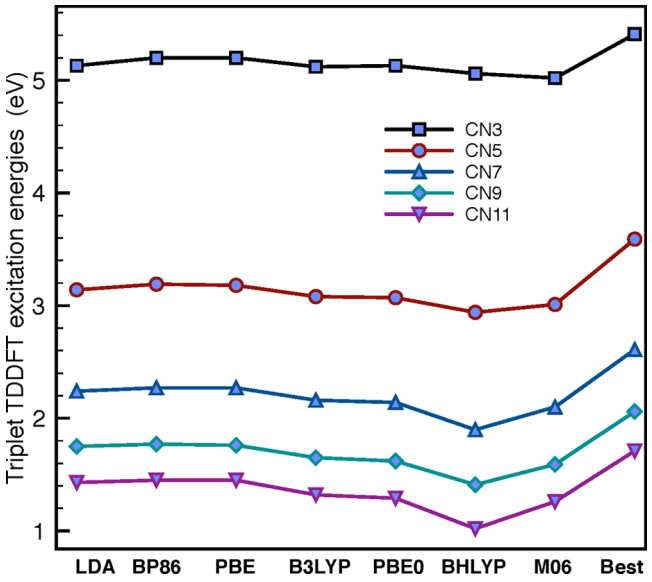

Figure 2. Triplet excitation energies calculated by TDDFT for CN($2k$ + 3) (k = 0, 4) based on seven functionals and the CC2 ab initio[31] benchmark "Best."

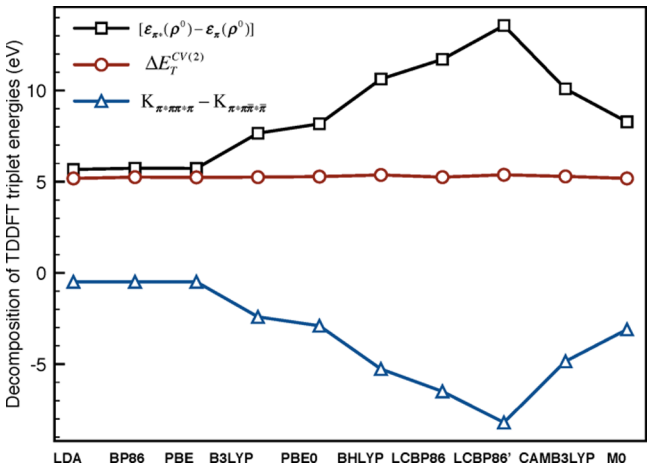

Figure 3. Decomposition of the triplet excitation energy for CN3 into the components introduced in eq 30.

instability of the ground state.[31] In the current study, ΔE_T^{TDDFT} is 0.3 eV below $\Delta E_T^{CV(2)}$ for BHLYP.

Turning next to the singlet energies, we display in Figure 4 the TDDFT singlet energies ΔE_S^{TDDFT} for CN($2k$ + 1) (k = 1, 5) based on nine different functionals in comparison to the CC2[31] bench mark. We find in agreement with other studies that the functional dependence of ΔE_S^{TDDFT} is minor and that the calculated values are above the *ab initio* values by 0.3 to 0.6

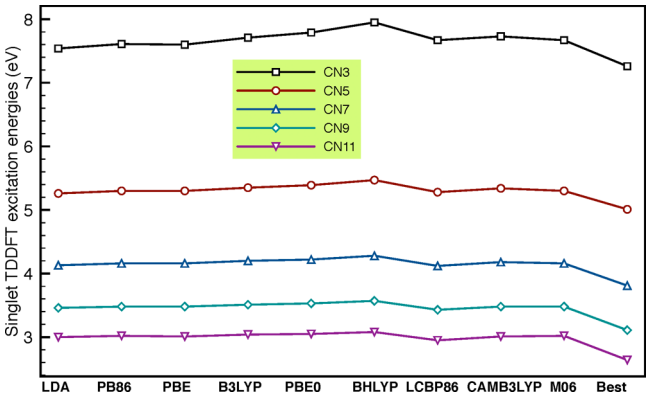

Figure 4. TDDFT singlet energies for CN($2k$ + 3) (k = 0,4) based on nine different functionals in comparison to the CC2 bench mark "Best."

eV depending on the adopted bench mark, Table 2. The calculated singlet energies $\Delta E_S^{CV(2)}$ based on eq 21 and the TD

Table 2. Coupled Cluster (CC2) Triplet and Singlet Excitation Energies (eV) for Cyanines

	ΔE_S[a,b]	ΔE_T[a,c]	ΔE_M[d]	$\Delta E_{S/T}$[e]
CN3	7.26[f]	5.41[g]	6.33	1.85
CN5	5.01	3.59	4.30	1.42
CN7	3.81	2.61	3.21	1.20
CN9	3.11	2.06	2.58	1.05
CN11	2.64	1.71	2.17	0.93

[a]Ref 31. [b]Singlet excitation energy. [c]Triplet excitation energy. [d]ΔE_M = 1/2(ΔE_S + ΔE_T). [e]Singlet triplet separation $\Delta E_{S/T}$ = (ΔE_S − ΔE_T). [f]Ref 29. [g]Extrapolated.

approximation are in general higher than ΔE_S^{TDDFT} by 0.5 eV or more. The functional dependence of $\Delta E_S^{CV(2)}$ is again minor in spite of the strong influence of α on the two components $[\varepsilon_{\pi^*}(\rho^0) - \varepsilon_{\pi}(\rho^0)]$ and $K_{\pi^*\pi\pi^*\pi} + K_{\pi^*\pi\bar{\pi}^*\bar{\pi}}$ that make up ΔE_S^{TDDFT}.

We display finally in Figure 5 the TDDFT singlet−triplet separation ΔE_S^{TDDFT} for the different cyanines and functionals compared to the CC2 "Best" values.[31] With ΔE_T^{TDDFT} being too low and ΔE_S^{TDDFT} too high, it comes as no great surprise that $\Delta E_{S/T}^{TDDFT} = \Delta E_S^{TDDFT} - \Delta E_T^{TDDFT}$ is firmly overestimated for all functionals studied here. The deviation between $\Delta E_{S/T}$ based on TDDFT and CC2 seems to grow with α and can reach more than 1 eV. The corresponding $\Delta E_{S/T}^{CV(2)}$ values are 0.5 eV above $\Delta E_{S/T}^{TDDFT}$, in line with the previous discussion and tend also to grow with α, albeit at a slower rate.

It follows from eq 22 that

dx.doi.org/10.1021/ct500292c | J. Chem. Theory Comput. XXXX, XXX, XXX−XXX

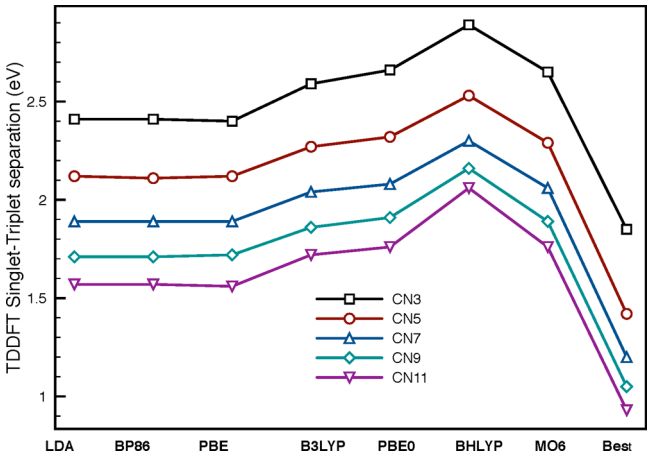

Figure 5. TDDFT singlet−triplet separations for the different cyanines and functionals compared to the CC2 "Best" values.

$$\Delta E_{S/T}^{CV(2)} \approx 2K^{C}_{\pi^*\pi\pi^*\pi} \tag{31}$$

This expression is in its form functional independent and the same for LDA and HF. Thus, any functional dependence comes indirectly through the way in which LDA and HF describe the (π,π^*) pair. It is well-known that LDA functions are more diffuse than HF orbitals due to the more slowly decaying LDA potential. It is thus not surprising that $2K^{C}_{\pi^*\pi\pi^*\pi}$ and $\Delta E_{S/T}^{CV(2)}$ will increase with α. Nevertheless, Figure 5 seems to indicate that the functional form for $\Delta E_{S/T}^{CV(2)}$ is inadequate, as already discussed previously.[31] Further, there can be little doubt that TDDFT is guilty as charged for overestimating the singlet−triplet separation in the cyanine $\pi \rightarrow \pi^*$ transitions, largely due to the inadequate representation given in eq 31.

4.2. Excitation Energies Based on ΔSCF and RSCF-CV(∞)-DFT. As already mentioned, variational methods based on static DFT have been applied to excited states for some time, even before the introduction of TDDFT, especially in the form of ΔSCF.[9] Thus, there have been several successful comparisons between experiment and ΔSCF studies on $\pi \rightarrow \pi^*$ transitions in dyes[39−41] using one or two functionals. In addition, Masunov[38] has developed a scheme that in our nomenclature would correspond to CV(4)-DFT and applied it to cyanines in conjunction with a solvation method. The comparison with experimental data is very promising. The objective of the present study is to conduct a systematic study on the performance of ΔSCF and RSCF-CV(∞)-DFT. However, because of the difficulty with comparing experimental absorption bands to calculated vertical transitions, we shall instead use wave function based *ab initio* results as benchmarks, as we did in our present TDDFT study above.

The excitations studied here can be described by a single $\pi \rightarrow \pi^*$ orbital replacement. In such cases the RSCF-CV(∞)-DFT and ΔSCF methods become identical, and the energy expressions put down in eq 23−26 are equally applicable for both schemes. However, for the description of several excitations within the same molecule, RSCF-CV(∞)-DFT is to be preferred since it avoids the variational collapses often encountered by ΔSCF. This is not an issue here, and we shall in the following cite ΔSCF. For singlet transitions involving a single orbital replacement, the two methods differ by less than 0.1 eV.[42,43] Unfortunately, a direct optimization of triplet excitations has not yet been implemented for RSCF-CV(∞)-DFT. We shall as a result in the following cite ΔSCF results.

We display the calculated triplet excitation energies of eq 23 ($\Delta E_T^{CV(\infty)} \approx \Delta E_T^{\Delta SCF}$) in Figure 6 for CN3−CN11 based on

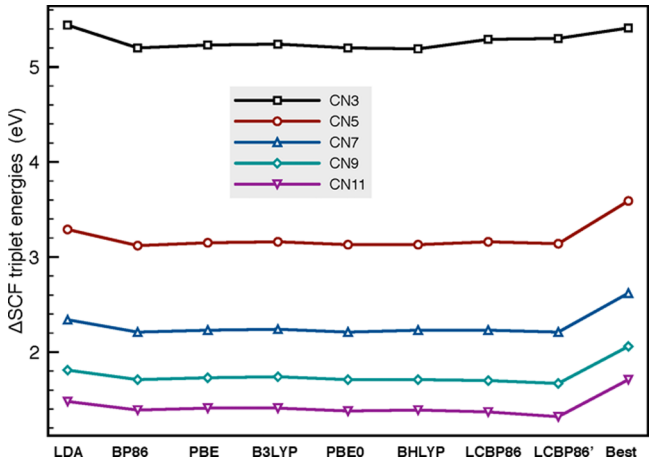

Figure 6. Calculated ΔSCF triplet excitation energies for CN3−CN11 based on eight different functionals.

eight different functionals. It is significant that all functionals for a given CN*n* afford very similar $\Delta E_T^{\Delta SCF}$ values, with LDA giving the largest deviation from the average of 0.1 eV. The similarity is even more striking when we note that the component making up $\Delta E_T^{\Delta SCF}$ in

$$\Delta E_T^{\Delta SCF} = [\varepsilon_{\pi^*}(\rho^0) - \varepsilon_{\pi}(\rho^0)] + \frac{1}{2}K_{\pi^*\pi^*\pi^*\pi^*} + \frac{1}{2}K_{\pi\pi\pi\pi} - K_{\pi^*\pi^*\bar{\pi}\bar{\pi}} + \Delta E_{Rel}^{T}(R) \tag{32}$$

exhibits considerable variations. This is illustrated for CN3 in Figure 7. We can rewrite the expression for $\Delta E_T^{\Delta SCF}$ by observing that the ionization potential of CN*n* in which an electron is ionized from the π−HOMO can be expressed as

$$IP_{\pi}(CNn) = -\varepsilon_{\pi}(\rho^0) + \frac{1}{2}K_{\pi\pi\pi\pi} \tag{33}$$

in the frozen orbital approximation where an electron is removed from the π−HOMO while keeping all other occupied orbitals the same as in the ground state. In a similar way, one can write the electron affinity $EA_{\pi^*}(CNn(+))$ of the π^*−LUMO for the CN*n*(+) system where one electron has been moved from π and one electron of the opposite spin added to π^* as

$$EA_{\pi^*}(CNn(+)) = -\varepsilon_{\pi^*}(\rho^0) - \frac{1}{2}K_{\pi^*\pi^*\pi^*\pi^*} + K_{\pi^*\pi^*\bar{\pi}\bar{\pi}} \tag{34}$$

where again use has been made of frozen ground state orbitals. Now we can write

$$\Delta E_T^{\Delta SCF} = IP_{\pi}(CNn) - EA_{\pi^*}(CNn(+)) + \Delta E_{Rel}^{T}(R) \tag{35}$$

It follows from Figure 8 that the different contributions $IP_{\pi}(CNn)$, $EA_{\pi^*}(CNn(+))$ and $\Delta E_{Rel}^{T}(R)$ all are remarkably insensitive to the functional used. Figure 8 underlines that for any functional, one can calculate electron affinities and ionization potentials in the Koopmann sense of frozen orbitals. Only, instead of using ground state orbital energies, one has to add "self-interaction" terms $K_{\pi^*\pi^*\pi^*\pi}$ and $K_{\pi\pi\pi\pi}$. These terms are not required in HF theory where they are zero, or in methods

dx.doi.org/10.1021/ct500292c | J. Chem. Theory Comput. XXXX, XXX, XXX−XXX

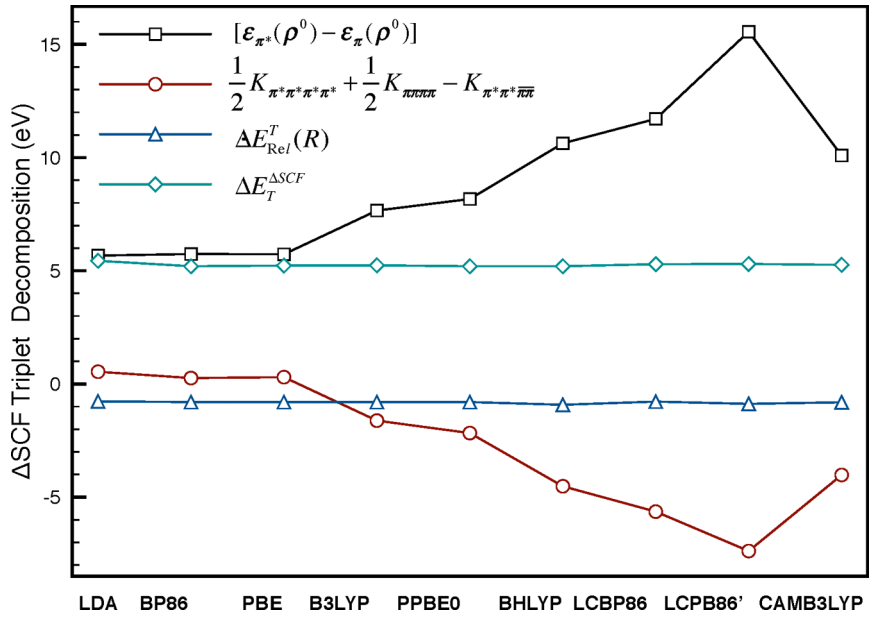

Figure 7. Decomposition according to eq 32 of ΔSCF triplet excitation energies for CN(3) based on eight different functionals.

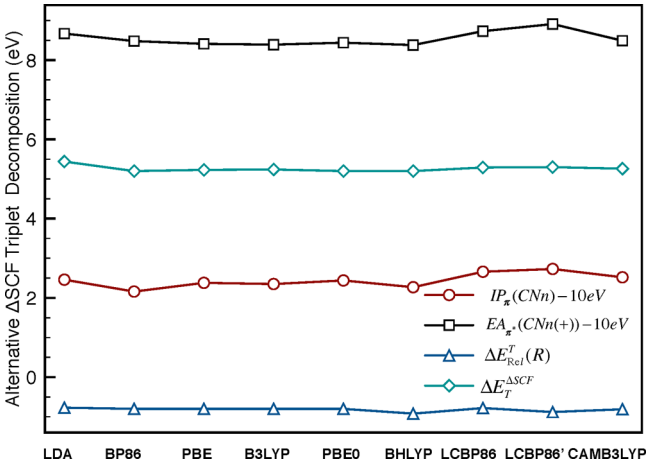

Figure 8. Decomposition according to eq 35 of ΔSCF triplet excitation energies for CN(3) based on eight different functionals.

with an "optimally tuned" functional where the frontier orbital energies are adjusted to correspond to −IP and −EA, respectively.[31] However, for all approximate functionals that do not use 100 % HF exchange, they are needed for $IP_{\pi}(CNn)$, $EA_{\pi^*}(CNn(+))$ and $\Delta E_T^{\Delta SCF}$. The formula in eq 33 is derived by writing $IP_{\pi^*}(CNn)$ in terms of the difference between two KS energies as $IP_{\pi}(CNn) = E_{KS}[\rho^0 - \pi\pi] - E_{KS}[\rho^0]$ and Taylor expand out from the ground state energy $E_{KS}[\rho^0]$ in powers of $\pi\pi$ up to two. We get in the same way eq 34 from $EA_{\pi^*}(CNn(+)) = E_{KS}[\rho^0 - \overline{\pi\pi}] - E_{KS}[\rho^0 - \overline{\pi\pi} + \pi^*\pi^*]$ by a Taylor expansion out from $E_{KS}[\rho^0]$ in powers of $\overline{\pi\pi}$ and $\pi^*\pi^*$ up to two.

We shall next turn to the singlet excitation energies $\Delta E_S^{\Delta SCF}$. They are based on eq 24 given by

$$\begin{aligned}\Delta E_S^{\Delta SCF} &= [\varepsilon_{\pi^*}(\rho^0) - \varepsilon_{\pi}(\rho^0)] + \frac{1}{2}K_{\pi^*\pi^*\pi^*\pi^*} + \frac{1}{2}K_{\pi\pi\pi\pi} \\ &\quad - 2K_{\pi^*\pi^*\pi\pi} + K_{\pi^*\pi^*\overline{\pi}\overline{\pi}} + \Delta E^{S}_{Rel}(R) \\ &= \Delta E_T^{\Delta SCF} + \Delta E_{S/T}^{\Delta SCF} \end{aligned} \quad (36)$$

We note from Figure 10 that they in contrast to $\Delta E_T^{\Delta SCF}$ are strongly functional dependent. It is further clear from our

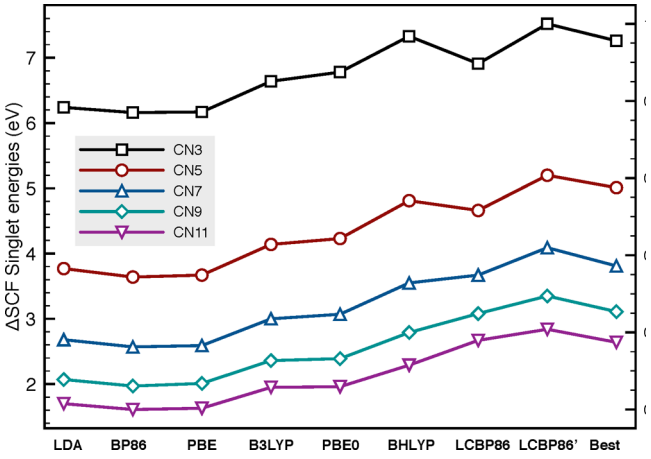

Figure 9. ΔSCF singlet energies for CN($2k + 3$) (k = 0,4) from eight different functionals in comparison to the CC2 bench mark "Best."

discussion so far that this dependency must come from the singlet−triplet separation $\Delta E_{S/T}^{\Delta SCF}$ since $\Delta E_T^{\Delta SCF}$according to Figure 7 is virtually functional independent. In eq 36, $\Delta E_{S/T}^{\Delta SCF}$ is according to eq 25 given by

$$\begin{aligned}\Delta E_{S/T}^{\Delta SCF} &= \Delta E_S^{\Delta SCF} - \Delta E_T^{\Delta SCF} \\ &= -2K_{\pi^*\pi^*\pi\pi} + 2K_{\pi^*\pi^*\overline{\pi}\overline{\pi}} + \Delta E^{S}_{Rel}(R) \\ &\quad - \Delta E^{T}_{Rel}(R) \\ &\approx -2K^{XC}_{\pi^*\pi^*\pi\pi} \\ &= -2(1-\alpha)K^{XC(KS)}_{\pi^*\pi^*\pi\pi} + 2\alpha K^{C}_{\pi^*\pi\pi^*\pi} \end{aligned} \quad (37)$$

where α is the fraction of HF exchange. Thus, since $0.0 < -K^{XC(KS)}_{\pi^*\pi^*\pi\pi} < K^{C}_{\pi^*\pi\pi^*\pi}$, we find as illustrated in Figure 9 that $\Delta E_{S/T}^{\Delta SCF}$ increases with the fraction α of HF exchange. This is in contrast to TDDFT, where $\Delta E_{S/T}^{TDDFT}$ is given by $K^{C}_{\pi^*\pi\pi^*\pi}$ for both local functionals and hybrides. We see in Table 1 that

dx.doi.org/10.1021/ct500292c | J. Chem. Theory Comput. XXXX, XXX, XXX−XXX

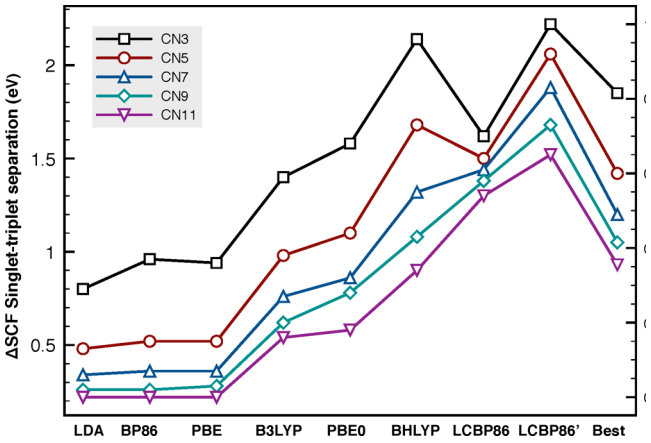

Figure 10. ΔSCF singlet−triplet separation energies for CN($2k$ + 3) (k = 0, 4) from eight different functionals in comparison to the CC2 benchmark "Best."

using a fraction as implemented in BHLYP affords a good agreement with CC2 and DMC and even better accord with exCC3. A fraction of α = 0.5 was also found to be optimal in a recent benchmark study on $\pi \rightarrow \pi^*$ transitions in conjugated hydrocarbons based on CV-DFT.[43]

5. CONCLUDING REMARKS

We have compared the performance of adiabatic time dependent density functional theory with (ATDFT/TD) and without (ATDFT) the Tamm Dancoff (TD) approximation to that of a time independent DFT scheme (ΔSCF) for the first $\pi \rightarrow \pi^*$ transition in a number of cyanine dyes using results from an *ab initio* coupled cluster (CC2) scheme as benchmark data. It is shown that the ATDDFT method affords too high singlet energies (ΔE_S^{TDDFT}) and too low triplet energies ΔE_T^{TDDFT} for all functionals. The singlet−triplet separations ($\Delta E_{S/T}^{TDDFT}$) are as a consequence consistently exaggerated. For (ATDDFT/TD), the $\Delta E_S^{TDDFT/TD}$ and $\Delta E_{S/T}^{TDDFT/TD}$ values are even more excessive. In ATDDFT/TD, the $\Delta E_{S/T}^{TDDFT/TD}$ term is given by a two-electron repulsion exchange integral between π and π^* ($K^C_{\pi^*\pi\pi^*\pi}$) and the same integral is the dominating contribution to $\Delta E_{S/T}^{TDDFT}$. It is thus understandable that $\Delta E_{S/T}^{TDDFT}$ and $\Delta E_{S/T}^{TDDFT/TD}$ only exhibit a weak functional dependence. It would further appear that the expression for $\Delta E_{S/T}^{TDDFT/TD}$ (and $\Delta E_{S/T}^{TDDFT}$) in terms of $K^C_{\pi^*\pi\pi^*\pi}$ is inadequate. Both ATDTDF/TD and ATDTDF have triplet energies that are functional independent and similar to ΔE_T^{TDDFT} and especially $\Delta E_T^{TDDFT/TD}$. On the other hand, both $\Delta E_S^{\Delta SCF}$ and $\Delta E_{S/T}^{\Delta SCF}$ are strongly functional dependent with values that increase with the fraction (α) of HF exchange included in a given functional. Both $\Delta E_S^{\Delta SCF}$ and $\Delta E_{S/T}^{\Delta SCF}$ are underestimated. However, for BHLYP with α = 0.5, we find $\Delta E_S^{\Delta SCF}$ to be in good agreement with available *ab initio* benchmarks. BHLYP has also previously been found to perform well in conjunction with ΔSCF and our kindred constricted variational DFT method for $\pi \rightarrow \pi^*$ transitions in conjugated hydrocarbons.[43]

The present study complements a recent[42] combined ΔSCF and RSCF-CV-DFT study on charge transfer where we also found that the triplet energies were nearly functional independent. However, in that case, the singlet−triplet separation was almost zero due to vanishing exchange integrals for both KS and HF. As a result, the singlet energies were also functional independent. It follows from the present study that singlet energies and singlet−triplet separations in general will be functional dependent and that it will be a challenge to find one functional that in general gives reliable estimates of $\Delta E_{S/T}^{\Delta SCF}$. However, our study also seems to indicate that $\Delta E_T^{\Delta SCF}$ can be obtained by simple local functionals such as LDA, PB86, and PBE. This opens for the possibility that $\Delta E_S^{\Delta SCF}$ can be obtained from a post-SCF determination of $\Delta E_{S/T}^{\Delta SCF}$ with a more advanced functional.

AUTHOR INFORMATION

Corresponding Author

*E-mail: ziegler@ucalgary.ca.

Notes

The authors declare no competing financial interest.

ACKNOWLEDGMENTS

T.Z. would like to thank the Canadian government for a Canada research chair in theoretical inorganic chemistry and NSERC for financial support. J.A. acknowledges support from the National Science Foundation, grant CHE-1265833.

REFERENCES

(1) Jensen, F. *Introduction to Computational Chemistry*; Wiley: New York,2006.
(2) Helgaker,T.; Jørgensen, P. and Olsen, J. *Molecular Electronic-Structure Theory*; Wiley: New York, 2000.
(3) Schreiber, M.; Silva-Junior, M.; Sauer, S.; Thiel, W. *J. Chem. Phys.* **2008**, *128*, 13411.
(4) Mata, R. A.; Werner, H.-J. *J. Chem. Phys.* **2006**, *125*, 184110.
(5) Høyvik, I. M.; Kristensen, K.; Jansik, B.; Jørgensen, P. *J. Chem. Phys.* **2012**, *136*, 014105.
(6) Riplinger, C.; Neese, F. *J. Chem. Phys.* **2013**, *138*, 034106.
(7) Runge, E.; Gross, E. K. U. *Phys. Rev. Lett.* **1984**, *52*, 997.
(8) Casida, M. E. In *Recent Advances in Density Functional Methods*; Chong, D. P., Ed.; World Scientific: Singapore, 1995; pp 155−193.
(9) Slater, J. C.; Wood, J. H. *Int. J. Quantum Chem. Suppl.* **1971**, *4*, 3.
(10) Elliott, P.; Goldson, S.; Canahui, C.; Maitra, N. T. *Chem. Phys.* **2011**, *391*, 110.
(11) Schipper, P. R. T.; Gritsenko, O. V.; van Gisberger, S. J. A.; Baerends, E. J. *J. Chem. Phys.* **2000**, *112*, 1344−1352.
(12) Likura, H.; Tsuneda, T.; Tanai, T.; Hirao, K. *J. Chem. Phys.* **2001**, *115*, 3540.
(13) Song, J.-W.; Watson, M. A.; Hirao, K. *J. Chem. Phys.* **2009**, *131*, 144108.
(14) Heyd, J.; Scuseria, G. E.; Ernzerhof, M. *J. Chem. Phys.* **2003**, *118*, 8207.
(15) Baer, R.; Neuhauser, D. *Phys. Rev. Lett.* **2005**, *94*, 043002.
(16) Dreuw, A.; Weisman, J.; Head-Gordon, M. *J. Chem. Phys.* **2003**, *119*, 2943.
(17) Tozer, D. *J. Chem. Phys.* **2003**, *119*, 12697.
(18) Cave, R. J.; Zhang, F.; Maitra, N. T.; Burke, K. *Chem. Phys. Lett.* **2004**, *389*, 39.
(19) Mazur, G.; Wlodarczyk, R. *J. Comput. Chem.* **2009**, *30*, 811.
(20) Casida, M. E. *J. Chem. Phys.* **2005**, *122*, 054111.
(21) Huix-Rollant, M.; Casida, M. E. cond-mat://arXiv.org/1008.1478.
(22) Romaniello, P.; Sangalli, D.; Berger, J. A.; Sottile, F.; Molinari, L. G.; Reining, L.; Onida, G. *J. Chem. Phys.* **2009**, *130*, 044108.
(23) Gritsenko, O.; Baerends, E. J. *Phys. Chem.* **2009**, *11*, 4640.
(24) Jacquemin, D.; Wathelet, V.; Perpète, E. A.; Adamo, C. *J. Chem. Theory Comput.* **2009**, *5*, 2420.
(25) Jacquemin, D.; Perpète, E. A.; Ciofini, I.; Adamo, C. *Acc. Chem. Res.* **2009**, *42*, 32634.
(26) Jacquemin, D.; Perpete, E. A.; Scuseria, G. E.; Ciofini, I.; Adamo, C. *J. Chem. Theory Comput.* **2008**, *4*, 123−135.

(27) Schreiber, M.; Buß, V.; Fülscher, M. P. *Phys. Chem. Chem. Phys.* **2001**, *3*, 3906−3912.
(28) Grimme, S.; Neese, F. *J. Chem. Phys.* **2007**, *127*, 154116.
(29) Send, R.; Valsson, O.; Filippi, C. *J. Chem. Theory Comput.* **2011**, *7*, 444−455.
(30) Jacquemin, D.; Zhao, Y.; Valero, R.; Adamo, C.; Ciofini, I.; Truhlar, D. G. *J. Chem. Theory Comput.* **2012**, *8*, 1255−1259.
(31) Moore, B., II; Autschbach, J. *J. Chem. Theory Comput.* **2013**, *9*, 4991−5003.
(32) Bertolino, C. A.; Ferrari, A. M.; Barolo, C.; Viscardi, G.; Caputo, G.; Coluccia, S. *Chem. Phys.* **2006**, *330*, 52.
(33) Champagne, B.; Guillaume, M.; Zutterman, F. *Chem. Phys. Lett.* **2006**, *425*, 105.
(34) Guillaume, M.; Liégeois, V.; Champagne, B.; Zutterman, F. *Chem. Phys. Lett.* **2007**, *446*, 165.
(35) Zhang, X.-H.; Wang, L.-Y.; Zhai, G.-H.; Wen, Z.-Y.; Zhang, Z.-X. *J. Mol. Struct. (THEOCHEM)* **2009**, *906*, 50.
(36) Bamgbelu, A.; Wang, J.; Leszczynski, J. *J. Phys. Chem. A* **2010**, *114*, 3551.
(37) Fabian. *J. Dyes Pigm.* **2010**, *84*, 36.
(38) Masunov, A. E. *Int. J. Quantum Chem.* **2010**, *110*, 3095.
(39) Ladame, S.; Spichty, M. *Dyes Pigm.* **2011**, *90*, 114.
(40) Yasarawan, N.; Thipyapong, K.; Ruangpornvisuti, V. *J. Mol. Struct.* **2011**, *1006*, 635.
(41) Toutchkine, A.; Han, W.-G.; Ullmann, M.; Liu, T.; Bashford, D.; Noodleman, L.; Hahn, K. M. *J. Phys. Chem. A* **2007**, *111*, 10849.
(42) Krykunov, M.; Ziegler, T. *J. Chem. Theory Comput.* **2013**, *9*, 2761.
(43) Ziegler, T.; Krykunov, M.; Cullen, J. *J. Chem. Phys.* **2012**, *136*, 124107.
(44) Cullen, J.; Krykunov, M.; Ziegler, T. *Chem. Phys.* **2011**, *391*, 11.
(45) Ziegler, T.; Seth, M.; Krykunov, M.; Autschbach; Wang, F. *J. Chem. Phys.* **2009**, *130*, 154102.
(46) Krykunov, M.; Seth, M.; Ziegler, T. *J. Chem. Phys.* **2014**, *140*, 18A502.
(47) (a) Ziegler, T.; Krykunov, M. *J. Chem. Phys.* **2010**, *133*, 074104. (b) Ziegler, T.; Seth, M.; Krykunov, M.; Autschbach, J.; Wang, F. *J. Chem. Phys.* **2008**, *129*, 184114.
(48) Hirata, S.; Head-Gordon, M. *Chem. Phys. Lett.* **1999**, *314*, 291.
(49) Amos, A. T.; Hall, G. G. *Proc. R. Soc.* **1961**, *A263*, 483.
(50) Martin, R. L. *J. Chem. Phys.* **2003**, *118*, 4775.
(51) te Velde, G.; Bickelhaupt, F. M.; van Gisbergen, S. J. A.; Fonseca Guerra, C.; Baerends, E. J.; Snijders, J. G.; Ziegler, T. *J. Comput. Chem.* **2001**, *22*, 931.
(52) Van Lenthe, E.; Baerends, E. J. *J. Comput. Chem.* **2003**, *24*, 1142.
(53) Vosko, S. H.; Wilk, L.; Nusair, M. *Can. J. Phys.* **1980**, *58*, 1200.
(54) Perdew, J. P.; Wang, Y. *Phys. Rev.* **1986**, *B 33*, 8822.
(55) Becke, A. D. *Phys. Rev.* **1988**, *A 38*, 3098.
(56) Becke, A. D. *J. Chem. Phys.* **1993**, *98*, 1372.
(57) Lee, C.; Yang, W.; Parr, R. G. *Phys. Rev.* **1988**, *B 37*, 785.
(58) Perdew, J. P.; Burke, K.; Ernzerhof, M. *Phys. Rev. Lett.* **1998**, *80*, 891.
(59) Ernzerhof, M.; Scuseria, G. *J. Chem. Phys.* **1999**, *110*, 5029.
(60) Adamo, C.; Barone, V. *J. Chem. Phys.* **1999**, *110*, 6158.
(61) Savin, A.; Flad, H.-J. *Int. J. Quantum Chem.* **1995**, *56*, 327−332.
(62) Akinaga, Y.; Ten-no, S. *Chem. Phys. Lett.* **2008**, *462*, 348−35.
(63) Akinaga, Y.; Ten-no, S. *Int. J. Quantum Chem.* **2009**, *109*, 1905−1914.
(64) Seth, M.; T. Ziegler, T. *J. Chem. Theory Comput.* **2012**, *8*, 901−907.
(65) Seth, M.; Ziegler, T.; Steinmetz, M.; Grimme, S. *J. Chem. Theory Comput.* **2013**, *9*, 2286−2299.
(66) Yanai, T.; Tew, D. P.; Handy, N. C. *Chem. Phys. Lett.* **2004**, *393*, 51.
(67) Grimm, B.; Dähne, S.; Bach, G. *J. Prakt. Chem.* **1975**, *317*, 161.